Chiang Mai J. Sci. 2017; 44(4) : 1487-1496
http://epg.science.cmu.ac.th/ejournal/
Contributed Paper

Synthesis of Cationic Polymer Coated Magnetite Nanoparticles Based on Poly(maleic anhydride-*alt*-1-octadecene)

Ong-art Thanetnit and Supawan Tantayanon*
Green Chemistry Research Laboratory, Department of Chemistry, Faculty of Science,
Chulalongkorn University, Phyathai Road, Pathumwan, Bangkok 10330, Thailand.
*Author for correspondence; e-mail: Supawan.T@chula.ac.th

Received: 24 August 2015
Accepted: 24 January 2016

ABSTRACT

We describe here the synthesis of aqueous dispersed cationic polymer coated magnetite nanoparticles. The cationic polymer was synthesized by two-steps reaction: the ring-opening reaction of commercial poly(maleic anhydride-*alt*-1-octadecene) (PMAO) with 2-(2-aminoethoxy)ethanol and subsequently grafting with glycidyltrimethylammonium chloride to obtain modified poly(maleic anhydride-*alt*-1-octadecene) (MPMAO). The characterization of MPMAO was determined by ATR-FTIR, ^{1}H and ^{13}C-NMR spectroscopy. By emulsion evaporation method, the magnetite nanoparticles prepared by the chemical co-precipitation were encapsulated with MPMAO to form modified poly(maleic anhydride-*alt*-1-octadecene) coated magnetite nanoparticles (MPMAO-Fe_3O_4 NPs). The average hydrodynamic diameter and ζ-potential value of MPMAO-Fe_3O_4 NPs were analyzed by dynamic light scattering measurement which found to be 43.2 nm and +29.3 mV, respectively. Thermogravimetric analysis, transmission electron microscopy and vibrating sample magnetometry of MPMAO-Fe_3O_4 NPs were also studied.

Keywords: cationic polymer, magnetite, magnetic nanoparticles, quaternization

1. INTRODUCTION

Magnetite nanoparticles (Fe_3O_4 NPs) have gained increasing attention because of their promising bio-applications including hyperthermia [1], magnetic resonance imaging [2], cell and bio-separation [3], drug targeting [4], magnetic transfections [5], tissue engineering [6] and chelating therapy [7]. Numerous chemical methods can be used to prepare Fe_3O_4 NPs such as chemical co-precipitation [8], microemulsion [9], sol-gel reaction [10], sonolysis [11], and hydrolysis and thermolysis of precursors [12]. However, Fe_3O_4 NPs are basically not stable under neutral condition in aqueous solution or in physiological fluid, resulting in agglomeration and precipitation. To improve the stability of Fe_3O_4 NPs and to avoid their aggregation, the surface modification of Fe_3O_4 NPs is thus necessary. Several approaches have been described for the preparation and

encapsulation of Fe_3O_4 NPs through the use of polymers [13], organic surfactants [14], inorganic metals [15] and bioactive molecules [16]. Among them, polymer coating has received much attention because it can serve as a good phase transfer agent as well as versatile platform for further applications, for example, the conjugation of nanoparticles to biological molecules.

The commercially available polymer, poly(maleic anhydride-*alt*-1-octadecene), PMAO, and its related polymers have been extensively employed as the phase transfer agents for transferring hydrophobic nanoparticles into water. Pellegrino *et al.* demonstrated water-soluble nanocrystals, $CoPt_3$, Au, CdSe/ZnS and Fe_2O_3, coated with PMAO-based polymer using bis (6-aminohexyl)amine as a cross-linker. Nanocrystals exhibited well dispersion in water upon hydrolyzation of the unreacted anhydride groups of PMAO coating [17]. Yu *et al.* reported the stabilization of Fe_3O_4 NPs and CdS/ZnS quantum dots, using PMAO-based polymer grafted with poly (ethylene glycol)methyl ether, which were very stable in water over pH 4-10 and physiological buffers [18,19]. Lees *et al.* also reported aqueous dispersion of polymer coated CdSe/ZnS quantum dots, which was formed by grafting Jeffamine M-100 polyetheramine onto poly(styrene-*co*-maleic anhydride). These nanocrystals exhibited long-term stability across pH 3-13 and showed the same optical spectra as those formed initially in organic solvents [20].

The surface modification of polymer can be accomplished by utilizing either a "grafting from" or a "grafting onto" methods. The first method required the nanoparticle surface owning the reactive functional groups to initiate the polymerization as well as the reaction under the complicated and sophisticated conditions. In contrast, the latter method basically utilized the reaction of functional groups on the polymer with the grafting agents. Advantageously, the grafting onto approach not only provides the simple pathway to carry out but also could generate a verities of the polymer modification.

Recently, polymeric nanoparticles carrying positive charges have been considered as a new medicine and gene therapy in the biomedical fields or utilized as an efficient microalgae carrier in the environmental applications. However, there are only a few reports on the stable aqueous dispersion of cationic polymer coated Fe_3O_4 NPs. Theppaleak *et al.* reported Fe_3O_4 NPs coated with the copolymer of poly(ethylene glycol) methyl ether methacrylate and diethylamino ethyl methacrylate *via* atom transfer radical polymerization (ATRP), followed by quarternization of the amino moiety in the diethylamino ethyl methacrylate units. The prepared positively charged nanoparticles led to better dispersion particles in water and improved the immobilizing efficiency of the PNA×DNA hybrids on their surface [21]. The cationic poly(2-(dimethylamino) ethyl methacrylate) (PDMA)-grafted Fe_3O_4 NPs *via in situ* ATRP, using 2-bromo-2-methylpropionic acid as an initiator, was reported [22]. The prepared nanoparticles was then able to assemble with negatively charged proteins, such as bovine serum albumin, which could enhance green fluorescent protein and were efficiently internalized by HeLa cells with low cytotoxicity under the external magnetic fields. Ge *et al.* reported the application of Fe_3O_4 NPs coated with a cationic PEI toward the separation of the biofuel-producing algae, *Scenedesmus dimorphus*. The PEI coating increased the harvesting of the algae and reduced dose demand of Fe_3O_4 NPs. The maximal levels of algal harvesting efficiency achieved by Fe_3O_4 NPs coated with PEI was approximately 83% [23].

In this work, the alternative approach for the synthesis of cationic polymer, MPMAO, as well as the polymeric magnetite nanoparticles, MPMAO-Fe_3O_4 NPs, were illustrated. By using the grafting onto approach, the cationic polymer was prepared by two step reactions which was started from the grafting reaction of the commercially available PMAO and 2-(2-aminoethoxy)ethanol and later reacted with glycidyltrimethylammonium chloride in a consequence. The formation and characterization of the MPMAO-Fe_3O_4 NPs was discussed in this paper.

2. MATERIALS AND METHODS

2.1 Materials Used

Poly(maleic anhydride-*alt*-1-octadecene) (PMAO, Mn= 30-50 kD), glycidyltrimethylammonium chloride, 2-(2-aminoethoxy)ethanol, ferrous chloride tetrahydrate, ferric chloride hexahydrate, and oleic acid were purchased from Sigma-Aldrich. Chloroform and ammonium hydroxide solution were obtained from ACI Labscan (Thailand) and Merck, respectively. All other reagents were used as received.

2.2 Synthesis of Fe_3O_4 NPs [24]

$FeCl_3 \cdot 6H_2O$ (24.3 g) and $FeCl_2 \cdot 4H_2O$ (12 g) were dissolved in 50 mL of deionized water under flowing nitrogen gas. NH_4OH (25%, 40 mL) was then added to the reaction mixture at 70-80°C. Oleic acid (40 %, w/w of formed magnetite) was added dropwise during 10 min and heated further for 30 min. After that, the temperature was raised to 110°C to remove water and excess NH_4OH. The black lump-like gel was separated by magnetic decantation and cooled to room temperature. After washing several times with deionized water and acetone, nanoparticles were dried at 30°C for 24 h and obtained as black powder.

2.3 Synthesis of Modified Poly(maleic anhydride-*alt*-1-octadecene) (MPMAO)

2-(2-Aminoethoxy)ethanol (0.86 mL) and PMAO (0.3 g) were added in $CHCl_3$ (3 mL). The solution was swirled at room temperature for 12 h and dialyzed with deionized (DI) water for 24 h. The polymeric solution was then freeze-dried, resulting in a yellowish powder, 0.36 g, named MPMAO precursor. MPMAO precursor (0.2 g) and glycidyltrimethylammonium chloride (90% in water, 0.74 mL) were added in buffer pH 7.4 (3 mL). The solution was stirred at room temperature for 48 h and dialyzed against DI water for 48 h. After lyophilization, the MPMAO was obtained as white powder, 0.23 g, named MPMAO.

MPMAO precursor. ^{1}H NMR (400 MHz, $CDCl_3$): δ 0.8 (br, CH_3-), 1.0-1.3 (br, C-CH_2-C), 3.2-3.6 (br, O-CH_2-C)

MPMAO. Solid State ^{13}C-NMR: δ 14.1 (br, CH_3-), 15.0-52.1 (br, C-CH_2-C), 54.7 (br, CH_3-N), 59.5-78.1 (br, O-CH_2-C, N-CH_2-C, O-CH-C), 169.5-187.9 (br, O=C-N, O=C-O)

2.4 Synthesis of MPMAO-Fe_3O_4 NPs

MPMAO in H_2O (0.2 mg/2mL) solution were dropwise in the Fe_3O_4 NPs in $CHCl_3$ (0.1 mg/2mL) and sonicated for 60 min. Then, chloroform was slowly removed by rotary evaporation. The solution was stirred at room temperature for 24 h. Aggregates were removed by centrifugation (twice, 15 min each). The excess MPMAO was removed from MPMAO-Fe_3O_4 NPs by ultracentrifugation (90,000 g for 1 h). The supernatant was discarded and MPMAO-Fe_3O_4 NPs re-suspended in water. After the solution was passed through a 0.2 μm nylon syringe filter, MPMAO-Fe_3O_4 NPs solution was obtained as brown filtrate.

2.5 Characterization Techniques

Size and shape of particles were determined using a transmission electron microscope (H-7650 Hitachi). The crystalline structure of particles was studied by an X-ray diffractometry system (operated with CuK_a radiation at 40 kV and 30 mA) and determined in the 2θ range from 10° to 80° (X-Ray Diffractometer (XRD) Model D8 Advance: Bruker AXS, Germany). Hydrodynamic diameter and ζ-potential of particles were measured by dynamic light scattering (DLS, Malvern Instruments Zetasier). Thermal gravimetric analysis (TGA) was performed by a TGA/SDTA 851e (Mettler-Toledo AG, Switzerland). The magnetic property of prepared NPs were determined using vibrating sample magnetometer (VSM, LakeShore 7404) at room temperature. ATR-FTIR spectra were obtained by a Bruker Vector 33 FT-IR spectrometer equipped with a DTGS detector. ^{1}H-nuclear magnetic resonance spectrum was recorded on a Varian Mercury NMR spectrometer. ^{13}C-solid state nuclear magnetic resonance spectrum was obtained using a nuclear magnetic resonance analyzer (Bruker-Advance, DPX-300 MAS-NMR).

3. RESULTS AND DISCUSSION

3.1 Synthesis of MPMAO

The cationic PMAO-based polymer was synthesized in two steps as shown in Scheme 1. The first step involved the ring opening reaction of the maleic anhydride moiety of PMAO with 2-(2-aminoethoxy)ethanol, at the mole ratio of 1:10, to obtain MPMAO precursor. The second step was the reaction of glycidyltrimethylammonium chloride, which inherently carried the positive charges, with hydroxyl group on MPMAO precursor, at the mole ratio of 5:1, to yield MPMAO. Similar approach utilizing glycidyltrimethylammonium chloride to introduce quaternary moieties had been reported in the preparation of quaternized polysaccharides such as chitosan [25].

MPMAO precursor and MPMAO were characterized by ATR-FTIR spectroscopic technique. Figure 1b exhibited ATR-FTIR spectrum of PMAO. It showed that the characteristic absorption bands at 1778 and 1706 cm^{-1}, and 1184 and 920 cm^{-1} were assigned to C=O stretching and C-O stretching of cyclic anhydride of PMAO, respectively. Figure 1c represented ATR-FTIR spectrum of MPMAO precursor which was similar to the one of PMAO, except the broad bands at 1702 and 1119 cm^{-1}, belonged to the C=O streching of amide and asymetrical C-O-C stretching of aliphatic ether, respectively. The broad band at 3600-3000 cm^{-1} was assigned to O-H stretching of unbounded hydroxy group of MPMAO precursor. All the other characteristic vibrations from MPMAO precursor corresponded to 2-(2-aminoethoxy)ethanol were also observed. In Figure 1d, ATR-FTIR spectrum of MPMAO showed a strong absorption band at 1466 cm^{-1}, which was attributed to the C-H bending of trimethyl ammonium group. The greater broad absorption band at 3600-3000 cm^{-1} was due to the increase in intramolecular hydrogen bonding between hydroxyl groups on cationic moiety of MPMAO.

The degree of substitution (DS) of MPMAO precursor was detemined by using ^{1}H-NMR spectroscopy as shown in the equation:

$$DS = \frac{\left(\frac{IH1}{8}\right)}{\left(\frac{IH2}{3}\right)}$$

where DS is the degree of substitution, IH1 is the intergral areas of the methylene protons of 2-(2-aminoethoxy)ethoxy moiety at 3.6-3.2 ppm and IH2 is the integral area

of methyl protons at 0.8 ppm. From the calculation, the DS of MPMAO precursor was found to be 0.85 indicating that 2-(2-aminoethoxy)ethoxy moiety were effectively grafted onto the maleic anhydride groups.

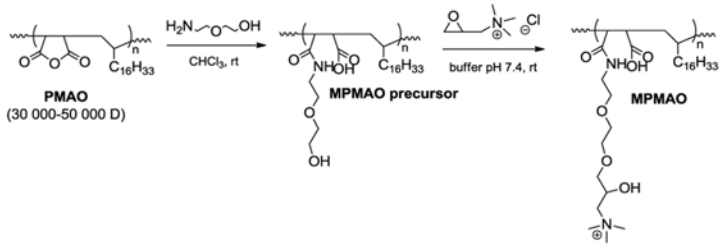

Scheme 1. Facile synthesis of MPMAO.

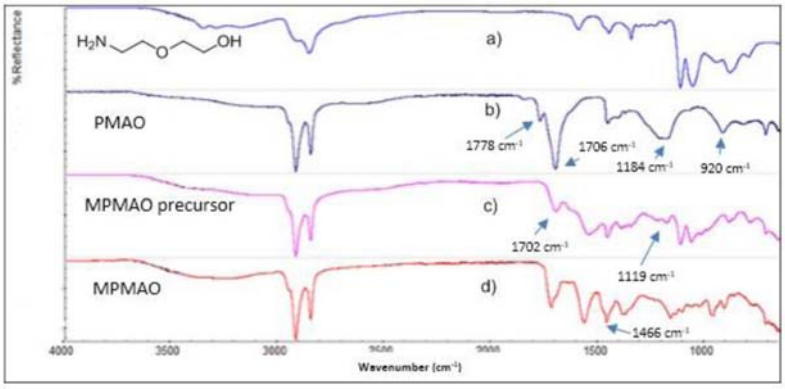

Figure 1. ATR-FTIR spectra of 2-(2-aminoethoxy)ethanol (a), PMAO (b), MPMAO precursor (c) and MPMAO (d).

Due to the increase in hydrophilicity of MPMAO, MPMAO could not dissolve in $CDCl_3$. Therefore, its identification was performed by solid state ^{13}C-NMR spectroscopic technique. Figure 3 represented the solid state ^{13}C-NMR spectrum of MPMAO. The characteristic carbons of the methyl groups of trimethyl ammonium unit was appeared at 54.7 ppm indicated the presence of quarternary ammonium moieties.

3.2 Synthesis of Fe_3O_4 NPs

Fe_3O_4 NPs were prepared by co-precipitation method and oleic acid was used as a surfactant. The crystalline structure of the synthesized Fe_3O_4 NPs was determined by X-ray diffraction (XRD) as shown in Figure 4. The six characteristic diffraction peaks at 2θ = 30.2° (d= 2.967 A°), 35.6° (d= 2.532 A°), 43.1°(d= 2.099 A°), 53.6° (d= 1.715 A°), 57.3° (d= 1.616 A°), 62.8° (d= 1.485 A°) were assigned to (220), (311), (400), (422), (511) and (440), respectively. By comparing the diffraction pattern of the sample with library data in the powder diffraction files using Diffrac-plus software, it revealed that the crystalline pattern matched with the standard pattern of Fe_3O_4 in isometric-hexaoctahedral crystal system.

The average diameter of the Fe_3O_4 NPs was determined to be 6.2 nm, calculated according to Scherrer's equation:

$$d = \frac{K\lambda}{\beta \cos\theta}$$

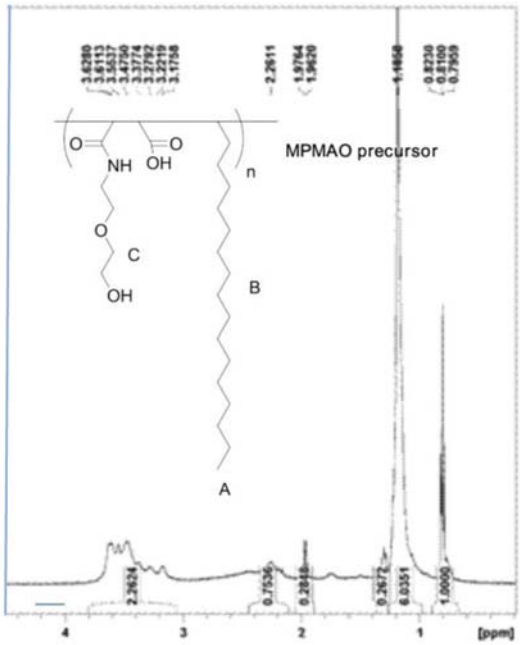

Figure 2. ^{1}H-NMR spectrum of MPMAO precursor in $CDCl_3$.

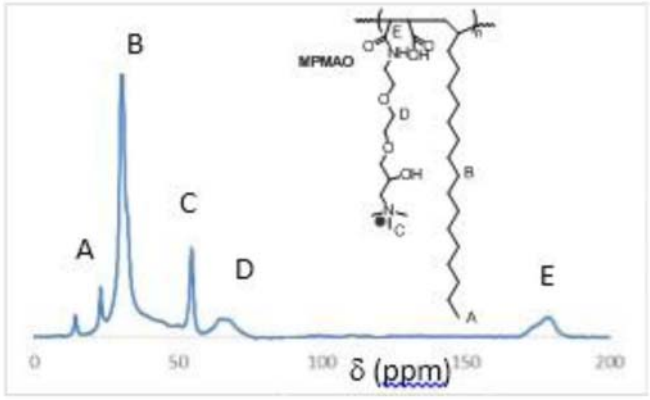

Figure 3. Solid state ^{13}C-NMR spectrum of MPMAO.

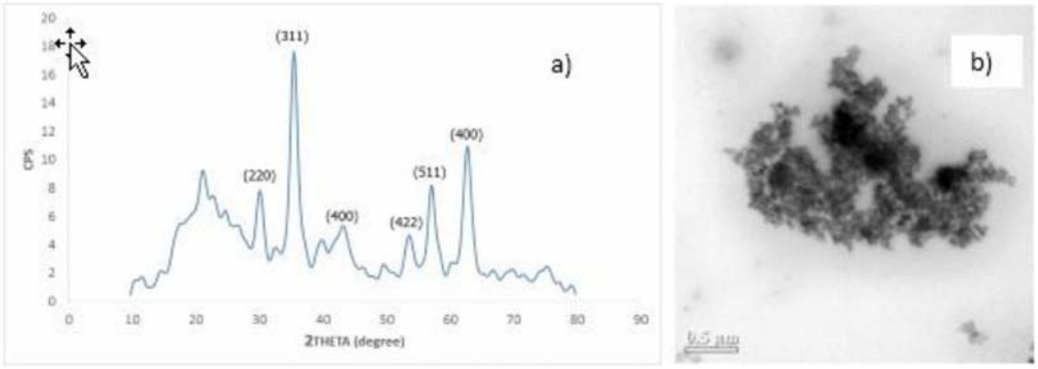

Figure 4. The XRD pattern (a) and TEM micrograph (b) of Fe_3O_4 NPs.

where d is the average size (nm), *K* is the shape factor, λ is the X-ray wavelength (nm), β is the width at half-maximun of the strongest peak (331) (radian) and θ is the Bragg's angle (radian). As revealed by TEM micrograph in Figure 4b, the morphology of the synthesized Fe_3O_4 NPs were apparently spherical particles. In addition, their average diameter were measured to be 9.8 ± 4.2 nm. Due to the average diameter less than 30 nm, the synthesized Fe_3O_4 NPs could presumally exhibit superparamagnetic property [24, 26 and 27].

3.3 Synthesis and Characterization of MPMAO-Fe_3O_4 NPs

The Fe_3O_4 NPs in chloroform were mixed with MPMAO in water then chloroform was gradually removed by rotary evaporation. MPMAO-Fe_3O_4 NPs were obtained as dispersion in water which significantly observed as brown solution.

The average of particle size of MPMAO-Fe_3O_4 NPs, as shown in TEM micrograph in Figure 5a, was found to be 10.8 ± 3.0 nm. It was about 10% larger than Fe_3O_4 NPs because of the determined polymer encapsulation onto Fe_3O_4 NPs. Figure 5b showed DLS size distribution graph of the MPMAO-Fe_3O_4 NPs in an aqueous media. The nanoparticles were relatively monodisperse in water. The obtained average hydrodynamic size of the colloidal MPMAO-Fe_3O_4 NPs was found to be 43.2 ± 12.9 nm, which was larger than the size measured by TEM. This difference was due to the coordination of the MPMAO outer layer of the particles with water which increased the particle size in aqueous media.

The ζ-potential measurement of MPMAO-Fe_3O_4 NPs was found to be +29.3 mV indicating the positive charges on the surface of nanoparticles. This was the reason why MPMAO-Fe_3O_4 NPs in aqueous solution showed well dispersion stability and did not agglomerate for over 2 months at room temperature because of the electrostatic replusion of the positive charges on the polymer coating surface.

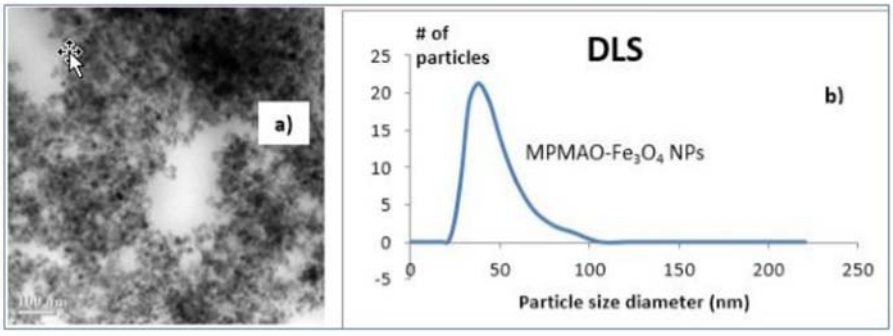

Figure 5. TEM micrograph (a) and particle size distribution curve (b) of MPMAO-Fe_3O_4.

Figure 6 represented TGA curves of Fe_3O_4 NPs and MPMAO-Fe_3O_4 NPs. As for TGA data of Fe_3O_4 NPs, oleic acid coated on the surface of Fe_3O_4 NPs was decomposed in the temperature range of 200-400°C, corresponding to 20.7 % weight loss and 79.3 % magnetite content. From TGA data of MPMAO-Fe_3O_4 NPs, the content of MPMAO coated on the surface of magnetite nanoparticles was calculated to be 22.5 %.

The magnetic property of Fe_3O_4 NPs and MPMAO-Fe_3O_4 NPs was determined at room temperature. From the VSM graphs

exhibited in Figure 7a and 7b, the saturation magnetization value of Fe_3O_4 NPs and MPMAO-Fe_3O_4 NPs were found to be 20.3 and 5.0 emu/g, respectively. The decrease in the saturation magnetization of MPMAO-Fe_3O_4 NPs compared to Fe_3O_4 NPs was due to the encapsulation of non-magnetic MPMAO on Fe_3O_4 NPs. After the removal of an external applied magnetic field, neither remanence nor coercivity was observed on the magnetic behavior of Fe_3O_4 NPs and MPMAO-Fe_3O_4 NPs indicating that both NPs exhibited superparamagnetic behavior at room temperature.

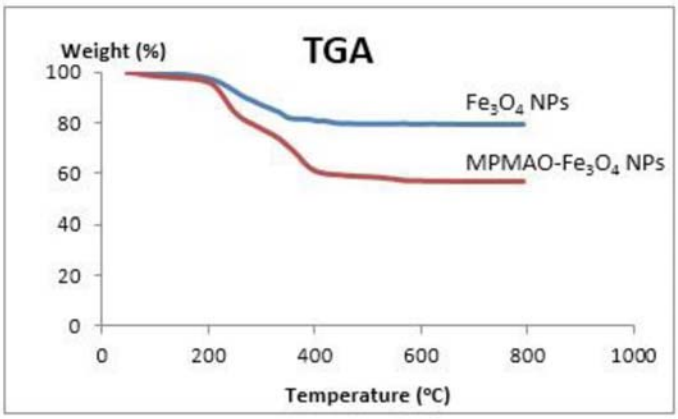

Figure 6. TGA curves of Fe_3O_4 NPs and MPMAO-Fe_3O_4 NPs.

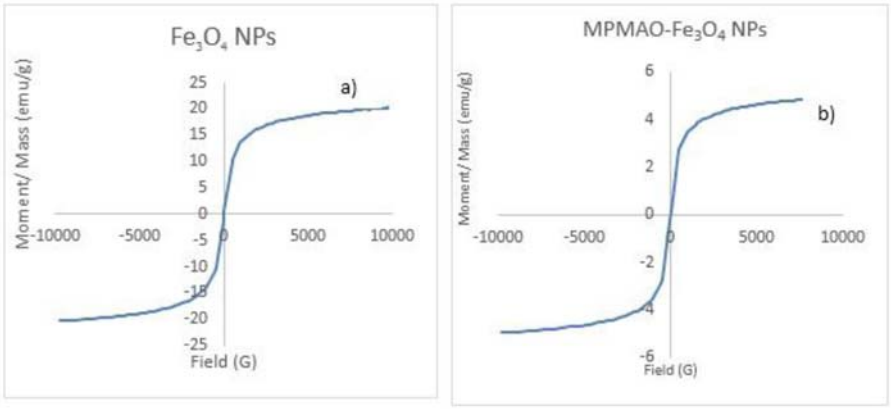

Figure 7. Magnetization curves of Fe_3O_4 NPs (a) and MPMAO-Fe_3O_4 NPs (b) at room temperature.

All the above results confirmed the synthesized cationic polymer coated Fe_3O_4 NPs based on PMAO. The schematic representation of dispersed MPMAO-Fe_3O_4 NPs was herein proposed as shown in Figure 8, which was similar to some other studies [19]. Oleic acid was coated over Fe_3O_4 NPs as primary layer, by using its carboxylic acid functional group bounded to the surface of Fe_3O_4 NPs and its long chain hydrocarbon positioned out of Fe_3O_4 NPs. Then, the hydrophobic site of MPMAO was bounded to the hydrocarbon chain of oleic acid, producing the second layer of the complex. The carboxylic acid group and cationic quaternary ammonium group were bonded to neighboring waters to make the nanoparticles well disperse in water.

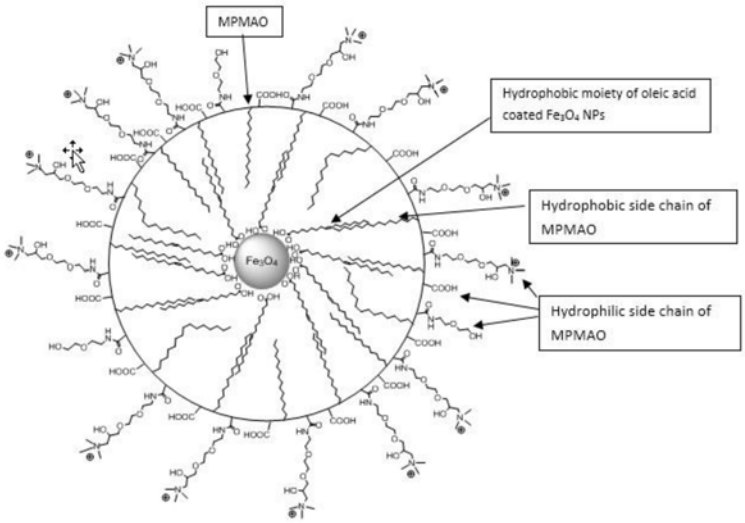

Figure 8. Schematic representation of dispersed MPMAO-Fe_3O_4 NPs.

4. CONCLUSIONS

The synthesis of the aqueous dispersed Fe_3O_4 NPs with cationic surface has been successfully demonstrated. It involved two simple reactions, the ring-opening of PMAO with 2-(2-aminoethoxy) ethanol and the grafting reaction of glycidyltrimethylammonium chloride to obtain the modified PMAO, which carried the cationic charges. With the commercial availability of several polyethylene glycols, the structure of the certain cationic polymer coated Fe_3O_4 NPs based on PMAO can be designed to suit the desired applications, for example, gene therapy and drug delivery in the biomedical fields. Accordingly, this work illustrated the greener synthesis to yield aqueous dispersed Fe_3O_4 NPs with positive charge which was less complicated than the other methods reported earlier.

ACKNOWLEDGEMENTS

The Scholarship from the Graduate School, Chulalongkorn University to commemorate 72nd Anniversary of his Majesty King BhumibalaAduladeja and Chulalongkorn University Fund are gratefully acknowledged. The authors are grateful to Chemistry and Biochemistry Department of Worcester Polytechnic Institute for some research facilities. The authors also thank Prof. William W. Yu and Prof. Jame W. Pavlik at Worcester Polytechnic Institute for their helpful suggestions and discussion.

REFERENCES

[1] Kikumori T., Kobayashi T., Sawaki M. and Imai T., *Breast Cancer Res. Treat.*, 2009; **113(3)**: 435-441. DOI 10.1007/s10549-008-9948-x.

[2] Zhang S., Liu X., Zhou L. and Peng W., *Mater. Lett.*, 2012. DOI 10.1016/j.matlet.2011.10.070.

[3] Das M., Dhak P., Gupta S., Mishra D., Maiti T.K., Basak A. and Pramanil P., *Nanotechnology*, 2010; **21(12)**: 125103-125114. DOI 10.1088/0957-4484/21/12/125103.

[4] Dong F., Guo W., Bae J.H., Kim S.H. and Ha C.S., *Chem. Eur. J.*, 2011; **17(45)**: 12802-12808. DOI 10.1002/chem.201101110.

[5] Wang X., Zhou L., Ma Y. and Gu H., *Nanotechnology*, 2009; **8(2)**: 142-147.

DOI 10.1109/TNANO.2009.2013946.

[6] Sapir Y., Cohen S., Friedman G. and Polyak B., *Biomaterial*, 2012; **33(16)**: 4100-4109. DOI 10.1016/j.biomaterials.2012.02.037.

[7] Daumann L.J., Larrabee J.A., Oillis D., Schenk G. and Gahan L.R., *J. Inorg. Biochem.*, 2014; **131**: 1-7. DOI 10.1016/j.jinorgbio.2013.10.007.

[8] LaMer V.K. and Dinegar R.H., *J. Am. Chem. Soc.*, 1950; **72(11)**: 4847-4854. DOI 10.1021/ja01167a001.

[9] Chin A.B. and Yaacob I.I., *J. Mat. Process. Technol.*, 2007; **191(1-3)**: 235-237. DOI 10.1016/j.jmatprotec.2007.03.011.

[10] Albornoz C. and Jacobo S.E., *J. Magn. Magn. Mater.*, 2006; **305(1)**: 12-15. DOI 10.1016/j.jmmm.2005.11.021.

[11] Kim E.H., Lee H.S., Kwak B.K. and Kim B.K., *J. Magn. Magn. Mater.*, 2005; **289**: 328-330. DOI 10.1016/j.jmmm.2004.11.093.

[12] Kimata M., Nakagawa D. and Hasegawa M., *Powder Technol.*, 2003; **132(2-3)**: 112-118. DOI 10.1016/S0032-5910(03)00046-9.

[13] Miles W.C., Huffstetler P.P., Goff J.D., Chen A.Y., Riffle J.S. and Davis R.M., *Langmuir*, 2011; **27(9)**: 5456-5463. DOI 10.1021/la105097d.

[14] Yi L.X., Yan T. and Lu G.G., *Sci. China Phys. Mech. Astron.*, 2011; **54(10)**: 1766-1770. DOI 10.1007/s11433-011-4481-z.

[15] Lee J., Lee Y., Youn J.K., Na H.B., Yu T., Kim H., Lee S.M., Koo Y.M., Kwak J.H., Park H.G., Chang H.N., Hwang M., Park J.G., Kim J. and Hyeon T., *Small*, 2008; **4(1)**: 143-152. DOI 10.1002/smll.200700456.

[16] Markova Z., Siskova K., Filip J., Safarova K., Prucek R., Panacek A., Kolar M. and Zboril R., *Green Chem.*, 2012; **9**: 2550-2558. DOI 10.1039/C2GC35545K.

[17] Pellegrino T., Manna L., Kudera S., Liedl T., Koktysh D., Rogach A.L., Keller S., Radler J., Natile G. and Parak W.J., *Nano. Lett.*, 2004; **4(4)**: 703-707. DOI 10.1021/nl035172j.

[18] Yu W.W., Chang E., Sayes C.M., Drezek R. and Colvin V., *Nanotechnology*, 2006; **17**: 4483-4487. DOI 10.1088/0957-4484/17/17/033.

[19] Yu W.W., Chang E., Falkner J.C., Zhang J., Al-Somali A.M., Sayes C.M., John J., Drezek R. and Colvin V.L., *J. Am. Chem. Soc.*, 2007; **129(10)**: 2871-2879. DOI 10.1021/ja067184n.

[20] Lees E.E., Nguyen T.L., Clayton A.H.A. and Mulvaney P., *ACS Nano.*, 2009; **3(5)**: 1121-1128. DOI 10.1021/nn900144n.

[21] Theppaleak T., Rutnakornpituk B., Wichai U., Vilaivan T. and Rutnakornpituk M., *J. Biomed. Nanotechnol.*, 2013; **9(9)**: 1-12. DOI 10.1166/jbn.2013.1645.

[22] Wang Z., Zhang J., Li R. and Chen J., *J. Appl. Polym. Sci.*, 2014; **131(10)**: 40260-40266. DOI 10.1002/app.40260.

[23] Ge S., Agbakpe M., Wu Z., Kuang L., Zhang W. and Wang X., *Environ. Sci. Technol.,* 2015. DOI 10.1021/es5049573.

[24] Hamoudeh M., Faraj A.A., Canet-Soulas E., Bessueille F., Leonard D. and Fessi H., *Int. J. Pharm.*, 2007; **338(1-2**): 248-257. DOI 10.1016/j.ijpharm.2007.01.023.

[25] Sajomsang W., Tantayanon S., Tangpasuthadol V. and Daly W.H., *Carbohyd. Res.*, 2009; **344(18)**: 2502-2511. DOI 10.1016/j.carres.2009.09.004.

[26] Bootdee K., Nithitanakul M. and Grady B., *Polym. Bull.*, 2012; **69(7)**: 795-806. DOI 10.1007/s00289-012-0773-3.

[27] Sun Z.X., Su F.W., Forsling W. and Samskog P.O., *J. Colloid Interf. Sci.*, 1998; **197(1)**: 151-159. DOI 10.1006/jcis.1997.5239.